J Polym Res (2015) 22: 14
DOI 10.1007/s10965-014-0651-9

ORIGINAL PAPER

Poly(pyridinium salt)s with organic counterions derived from 3,3′-dimethylnaphthidine: thermal, liquid crystalline, and optical properties

Robin Jose · Dat Truong · Haesook Han · Pradip K. Bhowmik

Received: 27 September 2014 / Accepted: 21 December 2014 / Published online: 29 January 2015

Abstract A poly(pyridinium salt) was synthesized from 4, 4′-(1,4-phenylene)bis(2,6-diphenylpyrilium)tosylate and 3, 3′-dimethylnaphthidine. Tosylate counterion was exchanged with other organic counterions such as triflimide, 1-napthalenesulfonate, and 2-napthalenesulfonate in DMSO to yield a total of four poly(pyridinium salt)s. Their chemical structures were established by using various spectroscopic techniques. Gel permeation chromatography showed that their number-average molecular weights (M_n) were in the range of 56–76 kg/mol and polydispersities in the range of 1.09–1.32. Their thermal stabilities ranged from 290 to 425 °C, under nitrogen atmosphere. Even though these polymers didn't show thermotropic liquid crystalline phases, counterion-dependent lyotropic liquid-crystalline phase were observed in some polar aprotic solvents above their critical concentrations. Each of these polymers emitted green light (500–572 nm) both in solutions and solid states as observed by UV–vis and photoluminescent spectroscopies.

Keywords Photoluminescent spectroscopy · Poly(pyridinium salt) · Ring transmutation polymerization · Ion exchange metathesis · Differential scanning calorimetry

Introduction

Poly(pyridinium salt)s are a class of ionic main-chain polymers that are usually prepared by ring-transmutation polymerization reaction of bispyrylium salts and diamines and by metathesis reactions. Depending on the chemical structures of bispyrylium salts and diamines, they can be π–conjugated or non-conjugated ionic polymers having interesting properties [1–14]. For example, some non-conjugated ionic polymers exhibit thermotropic liquid-crystalline (LC) and light-emitting properties in both solution and solid state [4, 5], others exhibit amphotropic LC and light-emitting properties in both solution and solid state [6–8]. Additionally, π-conjugated and even non-conjugated ionic polymers exhibit lyotropic LC properties in both protic and aprotic solvents and light-emitting properties in both solution and solid state depending on their chemical structures [9–14]. In this regard, they can be considered as functional ionic polymers. For example, one such poly(pyridinium salt) derived from calix[4]arene diamine was reported to have strong interactions with Pseudomonas fluorescens DNA, predominantly by electrostatic interactions as evaluated by fluorescent titration and transmission electron microscopy studies [15]. Another polymer prepared from benzidine giving rise to conjugated polyelectrolyte has been used to develop a sensitive fluorescence-based biosensor for homogeneous DNA detection [16]. Even a conjugated poly(pyridinium salt) based on 3,6-diamino-N-butylcarbazole exhibits aggregation-induced light emission characteristic up on which a fluorescence turn-on biosensor

Electronic supplementary material The online version of this article (doi:10.1007/s10965-014-0651-9) contains supplementary material, which is available to authorized users.

R. Jose (✉) · D. Truong
Department of Natural Sciences, University of Houston-Downtown, One Main Street, Houston, TX 77002-1001, USA
e-mail: Joser@uhd.edu

H. Han · P. K. Bhowmik (✉)
Department of Chemistry and Biochemistry, University of Nevada Las Vegas, 4505 Maryland Parkway, Box 454003, Las Vegas, NV 89154-4003, USA
e-mail: bhowmikp@unlv.nevada.edu

D. Truong
Department of Biochemistry and Biophysics, College of Agriculture and Life Sciences, Texas A&M University, 2128 TAMU, College Station, TX 77843-2128, USA

for calf thymus DNA detection and quantification has been developed [17].

Recently, we reported dispersing single-walled carbon nanotubes in dimethyl sulfoxide (DMSO) with poly(pyridinium salt)s via non-covalent interactions [18, 19]. Additionally, the 3,3′-dimethylnaphthidine is an interesting aromatic diamine that has been used for the preparation of polyamides and polyimides for functional applications. For example, this aromatic diamine in combination with suitable dianhydrides, e.g., spiroindane based dianhydides, is used for the preparation of intrinsic microporous polyimides with enhanced selectivity for membrane gas separations [20–23].

In this study, we describe the method of synthesizing four conjugated poly(pyridinium salt)s that incorporate 3,3′-dimethylnaphthidine moieties. They were prepared from 4, 4′-(1,4-phenylene)bis(2,6-diphenylpyrylium) tosylate and 3, 3′-dimethylnaphthidine by ring-transmutation polymerization reaction (**I**) followed by metathesis reaction (**II-IV**) with respective organic counterions. Scheme 1 shows the structures and designations of these poly(pyridinium salt)s (**I-IV**). The characterization of their chemical structures, lyotropic liquid crystalline, and light-emitting properties were performed by various experimental techniques including Fourier transform nuclear magnetic resonance (FTNMR), Fourier transform infrared (FTIR) spectroscopies, elemental analyses, gel permeation chromatography (GPC), differential scanning calorimetry (DSC), thermal gravimetric analysis (TGA), polarized light microscopy (PLM), and UV-Visible (UV–vis) and fluorescence spectroscopies.

Experimental

Materials and methods

Sodium 1-naphthalenesulfonate, sodium 2-naphthalenesulfonate, and lithium triflimide, were purchased from Sigma-Aldrich and used without further purification. The 2-methyl-1-naphthylamine was purchased from TCI America and concentrated H_2SO_4 was obtained from Fisher

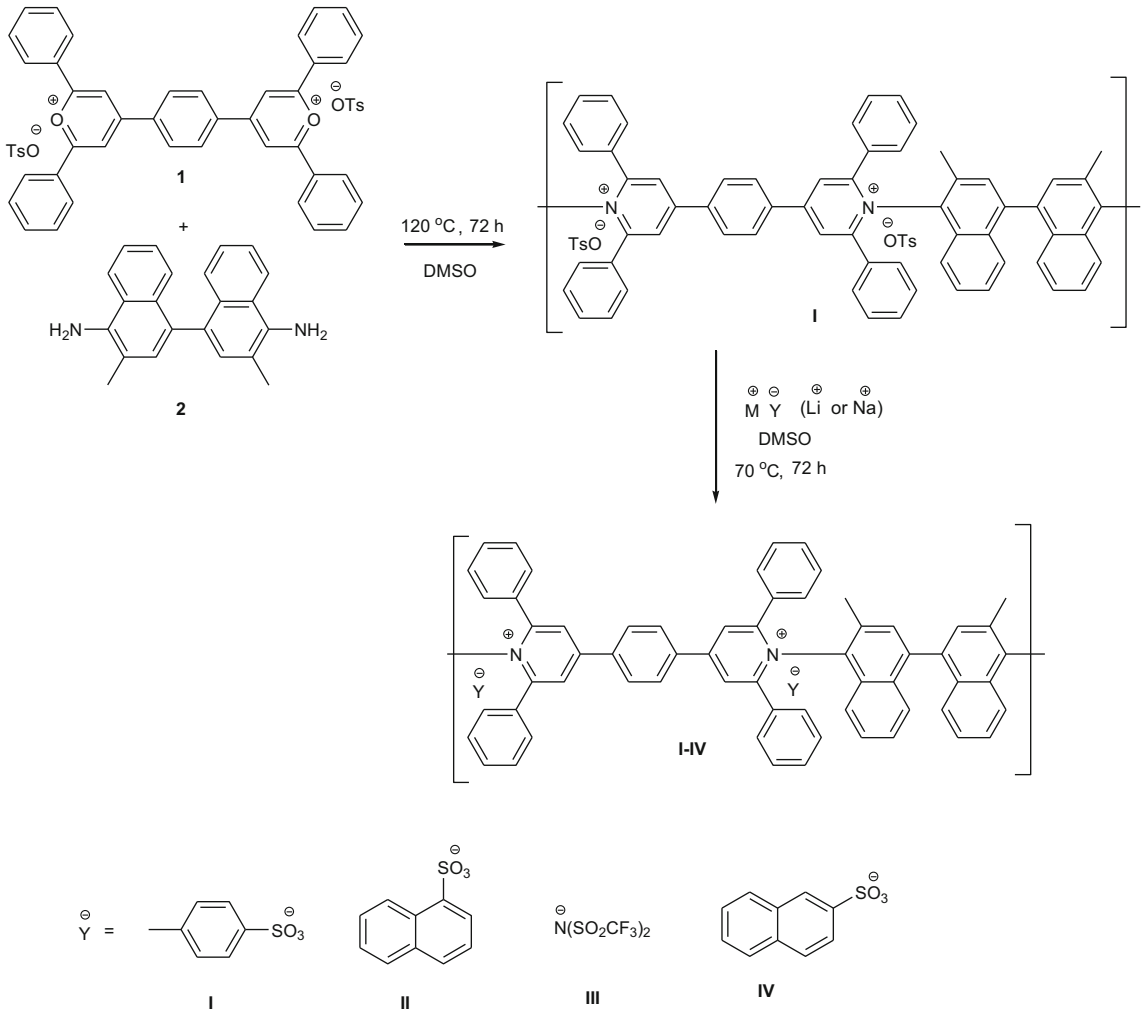

Scheme 1 Synthesis of poly(pyridinium salt)s by ring-transmutation polymerization

Scientific. All solvents used were obtained from Fisher Scientific and were HPLC grade. FTIR data was obtained using a Nicolet F530 spectrometer from films deposited on the IR plate from methanol solutions. The ^{1}H (300 MHz) and ^{13}C (75 MHz) NMR spectra were recorded using JEOL Eclipse spectrometer in DMSO-d_6 with TMS as an internal standard. Elemental analyses were performed by Atlantic Microlab in Norcross, GA. Pullulan standard P-50 used for the calibration of the GPC instrument was obtained from Polymer Standard Services USA, Inc. GPC was run at a flow rate of 1 mL/min at 50 °C. The GPC instrument was fitted with a Viscotek Model 301 Triple Detector Array which had a laser refractometer, a differential viscometer, and a light scattering detector (both right angle laser light scattering and low angle laser light scattering) in a single instrument and Water 515 pump. The array also had a fixed interdetector system and temperature control that can be regulated up to 80 °C. Separations were accomplished using ViscoGel I-MBHMW-3078 columns purchased from Viscotek. In a typical procedure, an aliquot of 100–200 μL of 2 mg/mL polymer solution in DMSO containing 0.1 M LiBr was injected. By injecting different volumes, the dn/dc values were corrected and the trend was assessed. Collected data was analyzed by Viscotek TriSEC software. TGA was performed with a Netzsch STA 409 CD using a 3–7 mg sample at a heating rate of 10 °C/min under helium atmosphere. DSC measurements were carried out using a Netzsch DSC 200 F3. Finely ground samples were placed in an aluminum pan and were heated and cooled at the rate of 10 °C/min under nitrogen atmosphere. Measurements were made in the temperature range of −30–200 °C. The resulting thermograms were analyzed above 25 °C using Netzsch Proteus software. The X-ray scattering studies were performed on finely ground samples at room temperature with a PANalytical X′PERT Pro X-ray diffraction spectrometer using Cu Kα radiation (λ=1.5419 Å) as an X-ray source operating at 45 kV and 40 mA. Lyotropic properties of these polymers were studied using polarized light microscopy (PLM) with a Laborlux 12 POL S polarizing light microscope equipped with crossed polarizers. The polymer samples were prepared in DMSO and acetonitrile at different concentrations and were equilibrated for 24–48 h. Samples were then placed between two cover slips and observed under the microscope. The photomicrographs were obtained using a Leica DFC425 C camera. These photomicrographs were analyzed using Leica Application Suite v.4.1 software. The UV–vis data was obtained in acetonitrile and methanol using Agilent Technologies Cary 60 UV–vis spectrometer. The fluorescence was measured in methanol and acetonitrile as well as in thin films using Fluoromax-4 spectrometer. Samples for thin-film measurements were prepared by evaporating dilute solutions of the corresponding polymers in quartz cuvettes.

Synthesis of monomers

The first monomer 4,4′-(1,4-phenylene)bis(2,6-diphenylpyrylium) tosylate, **1**, in Scheme 1 was synthesized from terepthalaldehyde and acetophenone in two-step procedure as reported in the literature [5]. The second monomer, **2**, in Scheme 1 was also synthesized based on a known procedure [4]. Briefly, in a round-bottomed flask fitted with a reflux condenser, 42 g of 68 % H_2SO_4 was taken and stirred using a magnetic stirrer. To this 5.00 g (0.0292 mol) of 2-methyl-1-naphthylamine was added dropwise. Sulfate salt of 2-methyl-1-naphthylamine precipitated which was heated to re-dissolve to give a red colored solution. The heating was continued for 48 h during that time the product precipitated out as pale pink solid. The reaction mixture was then cooled overnight, filtered and washed with de-ionized water and the solid wet cake was suspended in 100 mL water and heated with 200 mL of 1 M NaOH for 30 min and filtered. The collected solid was washed with de-ionized water and dried overnight. The crude product was then recrystallized from ethanol to give 2.25 g (49 % yield) of monomer **2**; mp: DSC peak maximum (T_m) at 216.1 °C. IR (film) (Fig. S1 in the Online Resources) ν (cm^{-1}): 3473.2, 3454.8, 3375.1, 3060.0, 2971.9, 229.6, 2857.1, 1617.3, 1573.5, 1458.2, 1415.5, 1373.4, 1264.9, 1245.3, 1181.9, 1161.8, 1134.0, 1099.8, 1031.6,1001.8, 948.7, 890.4, 869.6, 758.8.^{1}H NMR (Fig. S2 in the Online Resources) (300 MHz, DMSO-d_6, ppm) δ=8.20 (2H, d), 7.31 (2H, m), 7.07 (2H, s), 7.13 (4H), 5.44 (4H, s, NH_2), 2.30 (6H, s, CH_3).^{13}C NMR (Fig. S3 in the Online Resources) (75 MHz, DMSO-d_6, ppm) δ=141.12, 132.80, 132.20, 126.81, 126.58, 124.78, 124.01, 123.01, 122.71, 114.35, 18.51. Anal. (Calcd for $C_{22}H_{20}N_2$: C, 84.58 H, 6.45 N, 8.97. Found: C, 84.18 H, 6.71 N, 9.10 %).

Synthesis of polymer I

In a round bottom 3-neck flask fitted with a reflux condenser and a nitrogen purging assembly, 4.600 g (0.005200 mol) of **1** and 1.627 g (0.005210 mol) of **2** were taken. To this 50 mL of DMSO was added and heated at 120 °C for 72 h. The reaction mixture was then cooled to room temperature, the product precipitated from water, filtered, washed with copious amount of water, and dried under vacuum at 90 °C to give **I**. Its purity was determined from the ^{1}H NMR spectrum and elemental analysis. IR (film) ν (cm^{-1}): 3064, 2925, 1613, 1576, 1548, 1494, 1451, 1355, 1226, 1184, 1122, 1034, 1011, 922, 849, 818, 758, 700, 683.^{1}H NMR (300 MHz, DMSO-d_6, ppm) δ= 9.14 (4H, s), 8.82 (4H, s), 7.84 (4H, s), 7.45–7.47 (12H, br), 7.28 (12H, br), 7.07–7.09 (8H, m), 6.21 (2H, s), 2.33 (6H, s, tosylate), 2.27 (6H, s, CH_3). Anal. (Calcd for $C_{76}H_{58}N_2O_6S_2$: C, 78.73 H, 5.04 N, 2.42 S, 5.53. Found: C, 76.03 H, 4.97 N, 2.48 S, 5.40 %).

Syntheses of polymers II-IV

Polymer **I** was subjected to metathesis reaction with sodium 1-naphthalenesulfonate, lithium triflimide, and sodium 2-naphthalenesulfonate, respectively, to prepare polymers **II-IV**. In a typical procedure, **I** was dissolved in DMSO and to this a solution of the lithium or sodium salt of the respective counterion in DMSO was added and heated at 70 °C for 72 h. The mixture was then cooled to room temperature and the product was precipitated from excess water, filtered, washed with water, and dried under vacuum. This procedure was repeated three times to ensure complete exchange of ions verified by elemental analyses and ^{1}H NMR spectra. IR (film) for **II** ν (cm^{-1}): 3062, 2953, 1720, 1616, 1598, 1577, 1553, 1495, 1452, 1356, 1231, 1122, 1077, 1035, 922, 847, 756, 701, 673.^{1}H NMR (300 MHz, DMSO-d_6, ppm) for **II** δ=9.11 (4H, s), 8.84–8.81 (4H, m), 7.86–7.83 (12H, m), 7.51–7.40 (16H, m), 7.27–7.31 (14H, d), 6.21 (2H, s), 2.24 (6H, s, CH_3). Anal. (Calcd for **II**, $C_{82}H_{58}N_2O_6S_2$: C, 79.98 H, 4.75 N, 2.27. Found: C, 76.35 H, 4.80 N, 2.27 %). IR (film) for **III** ν (cm^{-1}): 3061, 1615, 1549, 1495, 1352, 1229, 1193, 1136, 1058, 844, 757, 699.^{1}H NMR (300 MHz, DMSO-d_6, ppm) for **III** δ=9.15 (4H, s), 8.82 (4H, s), 7.82 (4H, s), 7.49–7.28 (24H, br), 6.22 (2H, s), 2.25 (6H, s, CH_3). Anal. (Calcd for **III**, $C_{68}H_{44}F_{12}N_4O_8S_4$: C, 58.28 H, 3.16 N, 4.00 S, 9.15. Found: C, 57.14 H, 2.97 N, 3.99 S, 8.88 %). IR (film) for **IV** ν (cm^{-1}): 3061, 2835, 1722, 1616, 1598, 1577, 1553, 1495, 1453, 1357, 1231, 1202, 1080, 1037, 923, 848, 758, 701, 665.^{1}H NMR (300 MHz, DMSO-d_6, ppm) for **IV** δ=9.11 (4H, s), 8.83 (4H, s), 7.85–7.82 (12H), 7.70–7.27 (30H), 6.22 (2H, s), 2.23 (6H, s, CH_3). Anal. (Calcd for **IV**, $C_{82}H_{58}N_2O_6S_2$: C, 79.98 H, 4.75 N, 2.27. Found: C, 77.00 H, 4.76 N, 2.25 %).

Results and discussion

Chemical structures

Polymer **I** synthesized by a ring-transmutation polymerization was subjected to ion exchange metathesis in DMSO with counter ions 1-naphthalenesulfonate, triflimide, and 2-naphthalenesulfonate, respectively, to prepare polymers **II-IV**. Their chemical structures were established by FTIR,^{1}H NMR, and elemental analyses. Though polymers **II** and **IV** differ in their structures only by the position of the sulfonate group in the counterions, **II** appeared as a light fluffy powder and **IV** as a hard solid material. The FTIR spectrum of polymer **I** displayed characteristics tosylate ion peaks, among other peaks: 1122 (S=O asymmetric stretching), 1034 (S=O symmetric stretching), and 758 cm^{-1} (S–O stretching) as displayed in Fig. S4 in the Online Resources. Similarly, polymer **II** displayed characteristics 1-naphthalene sulfonate ion peaks, among other peaks: 1122 (S=O asymmetric stretching), 1035 (S=O symmetric stretching), and 756 cm^{-1} (S−O stretching) in its spectrum as displayed in Fig. S5 in the Online Resources. Polymer **III** displayed characteristics triflimide ion absorption peaks, among other peaks: 1352 (C−F stretching), 1136 (S=O asymmetric stretching), 1058 (S=O symmetric stretching), and 757 cm^{-1} (S–O stretching) as displayed in Fig. S6 in the Online Resources. The IR spectrum of polymer **IV** displayed characteristics 2-naphthalene sulfonate ion peaks, among other peaks: 1080 (S=O asymmetric stretching), 1037 (S=O symmetric stretching), and 758 cm^{-1} (S–O stretching) as displayed in Fig. S7 in the Online Resources. As reported for other ionic polymers found in literature, sulfonate counterion associated with organic cations showed symmetric bands at lower frequencies than those with inorganic cations suggesting weak ion-ion interaction between the organic counteranions and phenylated bipyridinium ions [4, 5, 24–26]. The^{1}H NMR spectrum of **I** showed chemical shift at δ=9.14 and 8.82 ppm for the protons of the aromatic moieties of poly(pyridinium salt). Chemical shift at δ=7.44, 7.07 and 2.33 ppm were assigned to the protons of the aromatic moiety and methyl group of the tosylate counterion. All other aromatic protons appeared as broad complex patterns in δ values of 6.21–7.84 ppm. In addition, the methyl protons of naphthidine moiety appeared at 2.27 ppm. Furthermore, the absence of vinylogous signals suggests that the ring-transmutation polymerization reaction underwent to completion. After exchange of counterion from tosylate to other organic counterions, the disappearance of tosylate peaks and appearance of new peaks of sulfonates indicated that the metathesis reaction also proceeded to completion under the experimental conditions used in **III-IV**. Because of the formation of viscous solutions of these polymers in DMSO,^{13}C NMR spectra could not be recorded for them even at elevated temperatures. High viscosities of their DMSO solutions coupled with broadness of their 1H NMR signals suggest high molecular weights of these polymers. The^{1}H NMR spectra of polymers **I-IV** are shown in Figs. S8–S11 in the Online Resources.

Molecular weights characterization

Since **I-IV** showed better solubility in DMSO than in other solvents, their number-average molecular weight (M_n) and polydispersity index ($PDI=M_w/M_n$) were measured in DMSO by GPC technique. Their number-average molecular weight (M_n) was in the range of 56–76 kg/mol and PDI values were between 1.09 and 1.31 (Table S1). After the completion of the metathesis reaction, their M_n and PDI values increased slightly in most cases suggesting that the weight and size of counterions affected their molecular weights.

Two other solution parameters, measured in DMSO at 50 °C, were also calculated: they are hydrodynamic radius,

R_h and radius of gyration, R_g. They were comparable to one another and in the range of 10.2–11.0 and 13.3–14.3 nm, respectively. These results and the narrow range of polydispersity index suggest that the effect of molecular weight on their solution, thermal, and optical properties are negligible.

Thermal properties

TGA thermograms displayed in Fig. 1 show relatively high thermal stabilities for the four ionic polymers. Furthermore, their thermal stabilities are influenced and varied by the structural nature of the counterions. Thus, they were found to have different thermal stability in the TGA thermograms. The lowest thermal stability was observed for **II** (290 °C) and the highest thermal stability was for **III** (425 °C). Polymers **I** (354 °C) and **IV** (362 °C) have intermediate decomposition temperatures in between **II** and **III**. The higher thermal stability of **III** than that of **I** is consistent with the previously reported results of other poly(pyridinium salt)s [1, 2]. It is interesting to note that **II** which appears soft and fluffy has less thermal stability than **IV** which appears like a hard solid (vide supra). The difference in thermal stabilities of **II** and **IV** also suggest that even minor changes in the structure of the counter ions can have profound influence on their thermal stabilities.

The DSC thermograms of polymers **I-IV** presented in Fig. 2 (second heating cycles) and Fig. S12 (second cooling cycles) in the Online Resources showed clearly T_g (also known as α transition) values in the heating and cooling cycles. Each of them showed a T_g ca. 103 °C in the heating cycle and 72 °C in the cooling cycle. In the heating cycles, there were additional low-temperature transitions that were attributed to β transitions, which were at 65, 44, 60, 50 °C, respectively, for polymers **I-IV**. Note here that the T_g values were independent of counterions, but the β transitions were dependent on counterions. The presence of only T_g in the heating and cooling cycles for each of these ionic polymers suggested that they were amorphous, which were verified by X-ray diffraction studies. Figures 3 and 4 show the X-ray powder diffraction (XRD) plots of polymers **I** and **IV**, respectively, recorded at room temperature. They show broad diffraction peaks with relatively low intensities at both small and wide angles, which are the characteristic features of amorphous phase of these ionic polymers. These peaks can be assigned to the intermolecular short-range interactions that are parallel and perpendicular to the long axes of the polymer chain. The broad wide-angle diffraction peaks at around 2 = 21.05° in case of polymer **I** and 2 =21.67° in case of polymer **IV** that corresponded to the *d*-spacings of 4.2 and 4.1 Å, respectively, are the distances of two aromatic planes of the polymer chains. The relative sharp, wide-angle diffraction peaks at around 2 =11.29° in case of polymer **I** and 2 = 10.27° in case of polymer **IV** that corresponded to the *d*--spacings of 7.8 and 8.6 Å are related to long-range order between the polymer chains.

Lyotropic properties

Polymers **I-IV** formed lyotropic LC phases in DMSO at relatively low concentrations at room temperature as shown in Fig. 5. The critical concentrations of polymers **I** and **III** were 15 wt% in DMSO and that of polymer **II** was 10 wt% in DMSO. At these critical concentrations, they exhibited biphasic solutions wherein there coexisted an anisotropic (LC) and isotropic phase when examined with a PLM under crossed polarizers. With further increase in concentration, each of them exhibited a fully-grown lyotropic phase at ca. 25 wt% in this solvent. Interestingly, polymer **IV** containing 2-naphthelenesulfonate appeared to form biphasic solutions

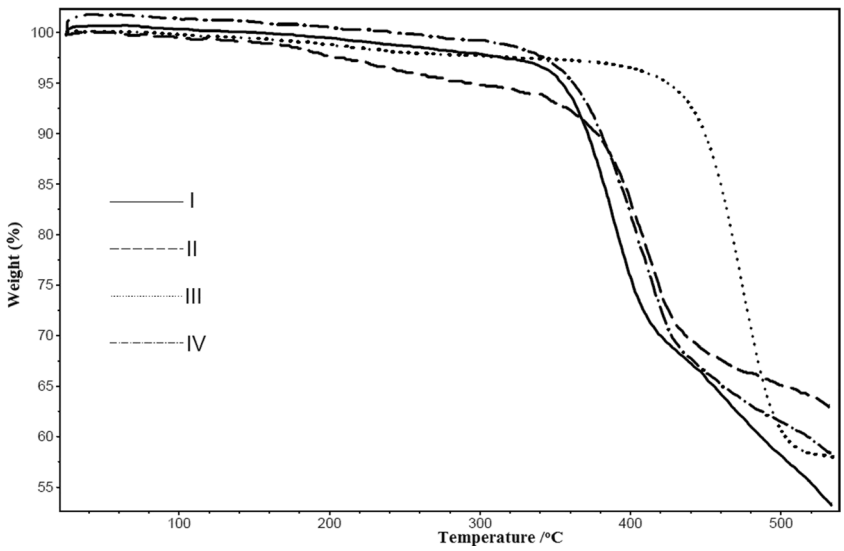

Fig. 1 TGA thermograms of polymers I-IV obtained at the heating rate of 10 °C/min under helium

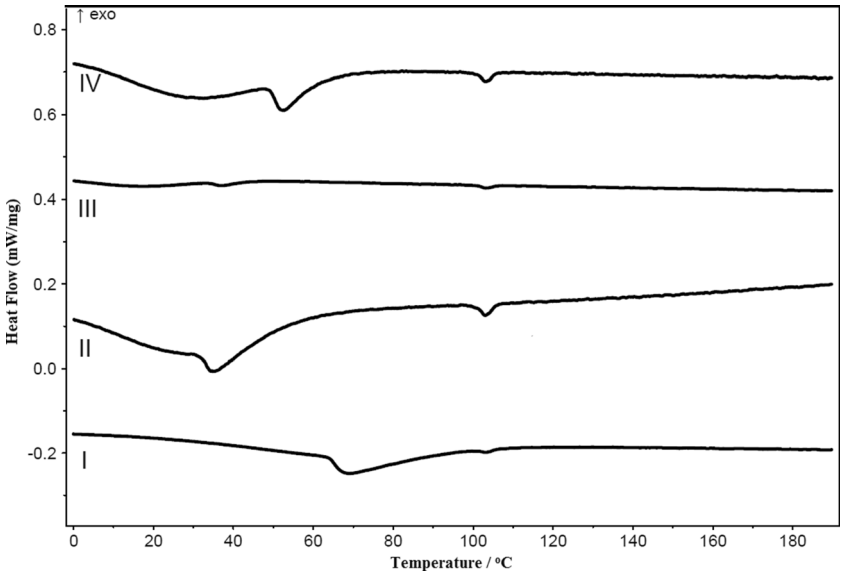

Fig. 2 DSC thermograms of polymers I–IV in the second heating cycles at the rate of 10 °C/min under nitrogen

(Fig. 5g) with polymer forming ribbon-like morphology over the concentration range of 10–20 wt% in DMSO when observed using a PLM under crossed polarizers. The intensity of birefringence of biphasic solutions as well as the number of ribbon like structures increased with polymer concentration in this solvent (Fig. 5h). These results are in excellent agreements with the lyotropic properties of other poly(pyridinium salt)s [1, 8, 9, 14]. It can be assumed that the position of the sulfonate group in 2-napthalenesulfonate counterion helps to induce these ribbon-like formations in **IV**.

Polymer **III** had the best solubility in acetonitrile among the polymers in the series. It showed isotropic, biphasic, and lyotropic solutions at 3, 5, and 10 wt% in this solvent. Its critical concentration was lower than that in DMSO (Fig. 6a). These results are consistent with those of other lyotropic LC forming poly(pyridinium salt)s [1, 8, 9, 14]. Polymers **I**, **II**, and **IV** had low solubility in this solvent. However, 10 wt% of **I** had sufficient interactions in this solvent to form biphasic solutions in which gelled polymer showed birefringence as shown in Fig. 6c. Polymers **II** and **IV** with naphthalene sulfonate counter ions had very minimum interaction with this solvent and exhibited phase separation. However, when the solvent-swelled polymer sample was observed with a PLM under crossed polarizers, it showed birefringence as shown in Fig. 6d and e, respectively. Like in DMSO, polymer **IV** also formed ribbon-shaped birefringence as shown in Fig. 6f. In general, sufficient solubility and rod-like backbone that facilitates the alignment of the polymer chain favors LC phase formation in polymer solutions [27]. Solubility and backbone structure are further

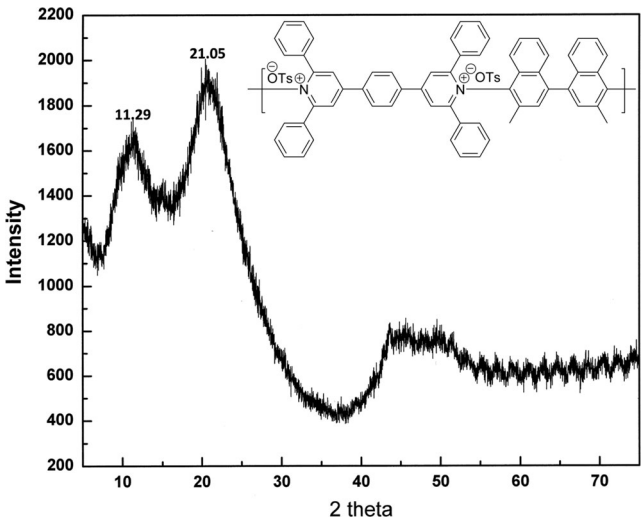

Fig. 3 X-ray powder diffraction plot of polymers I recorded at room temperature

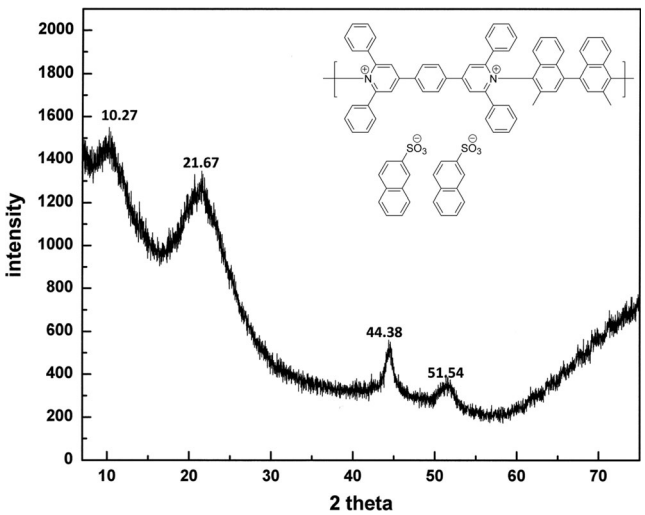

Fig. 4 X-ray powder diffraction plot of polymers IV recorded at room temperature

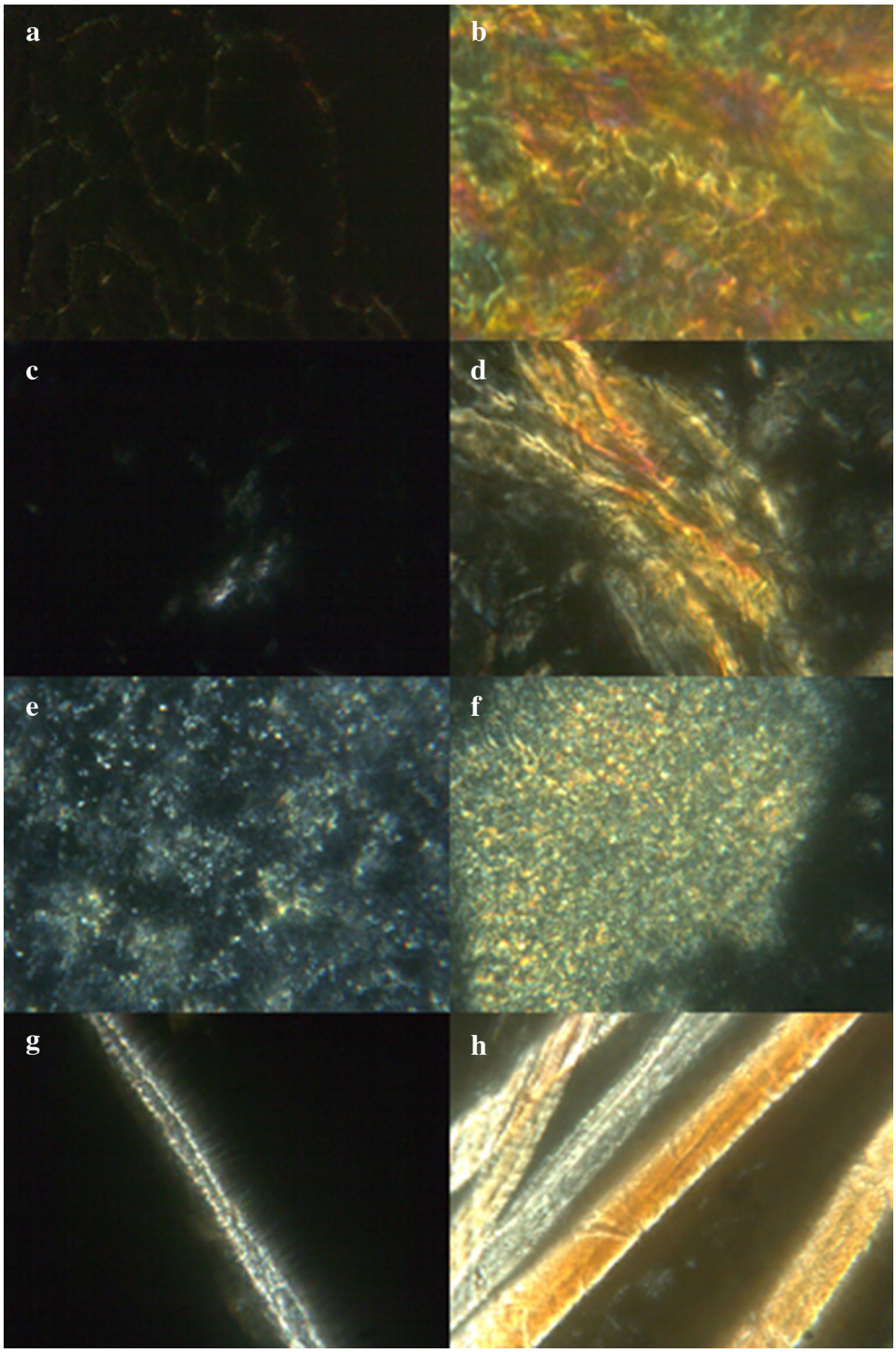

Fig. 5 Photomicrographs of polymers I-IV in DMSO taken at room temperature under crossed polarizers showing lyotropic LC phases (magnification 50×). **a** I–15 wt% in DMSO; **b** I–25 wt% in DMSO; **c** II–10 wt% in DMSO; **d** II–25 wt% in DMSO; **e** III–15 wt% in DMSO; **f** III–25 wt% in DMSO; **g** IV–10 wt% in DMSO; **h** IV–20 wt% in DMSO

dependent on the structure of the monomers, molecular weight, temperature, and the interaction of the polymer chain with solvent and other polymer chains [28].

Therefore, the presence of organic counterions and their nature in **I-IV** can influence any of these factors thus favoring the of formation of lyotropic phases in DMSO and acetonitrile.

Optical properties

Because of the presence of organic counterions in combination with phenylated pyridinium moieties and rigid 3,3′-dimethyl naphthidine moieties, these ionic polymers showed good solubility in DMSO, but their light-emission properties in this solvent were very weak. However, their solubility in

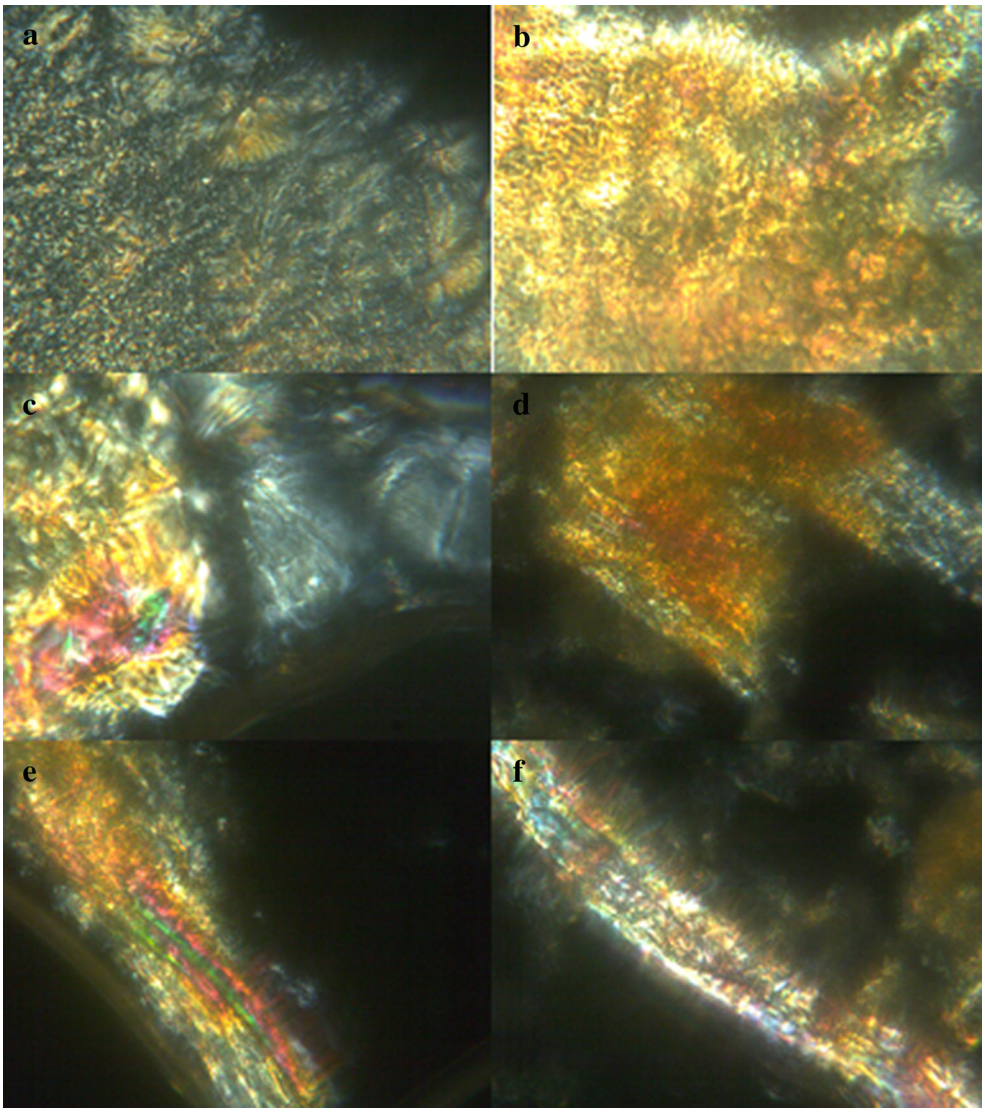

Fig. 6 Photomicrographs of polymers I-IV in acetonitrile taken at room temperature under crossed polarizers (magnification 50×). **a** III–5 wt% in ACN; **b** III–15 wt% in ACN; **c** I–10 wt% in ACN; **d** II–solvent swelled polymer in ACN; **e** IV–solvent swelled polymer in ACN; **f** IV–solvent swelled polymer in ACN showing ribbon like formation

acetonitrile and methanol was sufficient enough that enabled us to measure their optical properties in solutions and in thin-film states cast from these solvents by UV–vis and photoluminescent (PL) spectroscopies. Each of the polymers **I-IV** showed essentially an identical λ_{max} in the narrow range of 329–344 nm as measured in its absorption spectra recorded in acetonitrile and in a narrow range of 345–346 nm in methanol (Figs. S13 and S14, respectively, in the Online

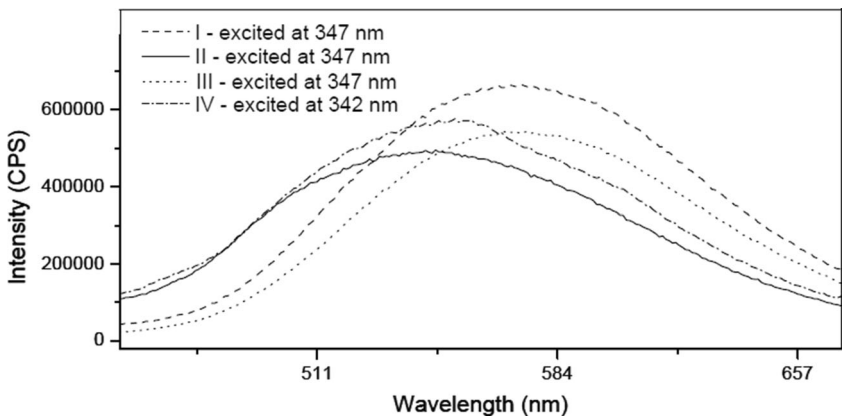

Fig. 7 Emission spectra of polymers I-IV in acetonitrile excited at various wavelengths

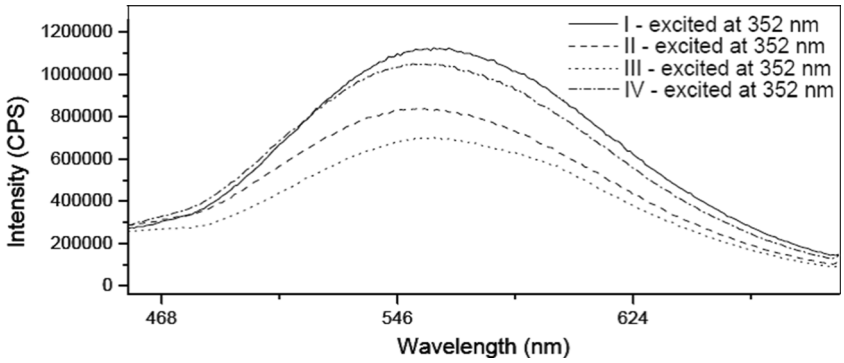

Fig. 8 Emission spectra of polymers I-IV in methanol excited at fixed wavelength

Resources). These results suggest that their absorption maxima were less sensitive to the polarities of the solvents examined. In other words, the interactions of acetonitrile and methanol with the polymer backbone did not cause any changes in the energies of their ground states. The optical band gaps (E_g) of these polymers were found to be 3.32 eV in acetonitrile and 3.27 eV in methanol as determined from the onset of wavelength in each of the UV–vis absorption spectra. These E_g values are similar to other poly(pyridinium salt)s found in literature [4–6, 14], but higher than those of π–conjugated light-emitting polymers [29, 30].

Optical properties of polymers **I-IV** in acetonitrile and methanol and solvent-cast thin films from these solvents are summarized in Table S2 in the Online Resources. Figure 7 shows the emission spectra of these polymers in acetonitrile at various excitation wavelengths of light, each of which consists of a broad, distinct λ_{em} peak with no vibrational structures. Their λ_{em} peaks were also dependent on the nature of the counterions. **I** and **III** showed an identical λ_{em} peak at 572 nm; and **II** and **IV** showed an emission peak at 543 nm, when excited at various excitation wavelengths of light, in a relatively polar aprotic solvent like acetonitrile. In protic polar solvent like methanol, they showed an identical λ_{em} peak at 556 nm, when excited at fixed wavelength of light (Fig. 8 and Table S2). Thus, it appeared that **I** and **III** showed a hypsochromic shift of 16 nm when compared to that in acetonitrile. In contrast, **II** and **IV** showed a bathochromic shift of 13 nm in this solvent when compared to that in acetonitrile. The fwhm value for each of the emission spectra of these polymers is also quite broad, indicative of light-emission from a number of chromophoric species.

The films of these polymers **I-IV** were prepared from their respective solutions (acetonitrile or methanol) casting onto quartz cuvettes. Their solid-state emission spectra cast from acetonitrile and methanol are shown in Figs. 9 and 10 respectively. In thin films when cast from acetonitrile solutions, all of these polymers showed a broad λ_{em} peak in their emission spectra with the complete loss of vibrational fine structures at 511 nm when excited at 347, 357, 357 and 342 nm wavelengths of light, respectively (Fig. 9). Similarly, when their films were cast from methanol, they also showed a broad λ_{em} peak in their emission spectra with the complete loss of vibrational fine structures at 511, 500, 511, and 511 nm when excited at 367, 362, 357 and 362 nm light, respectively (Fig. 10). On changing from solutions to the thin films cast from acetonitrile, **I-IV** showed large hypochromic shifts of 61, 32, 61 and 32 nm, respectively, in their λ_{em} values, when compared to those of their solutions spectra. Similarly, in thin films cast from methanol, **I-IV** showed large hypochromic shifts of 45, 56, 45 and 45 nm, respectively, in their λ_{em} values, when compared to those of solutions spectra. The fwhm values of emission spectra in thin films of these polymers cast from both acetonitrile and methanol were relatively narrower when compared to those in their solutions spectra in

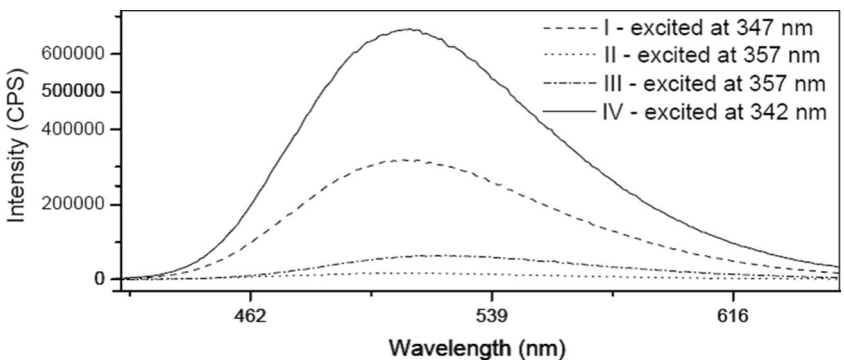

Fig. 9 Emission spectra of polymers I-IV in films cast from acetonitrile at various excitation wavelengths

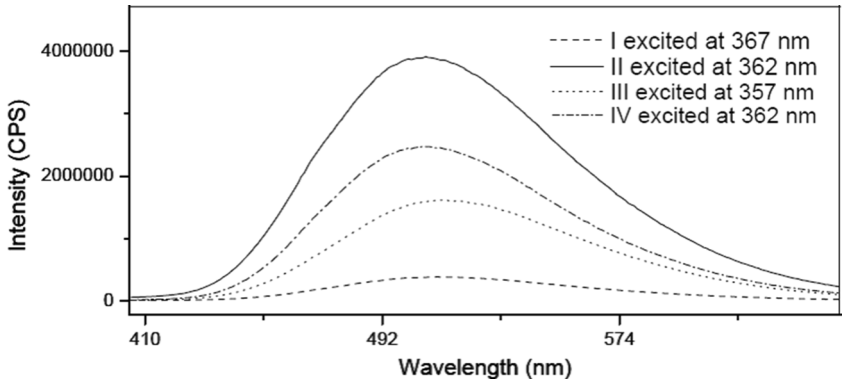

Fig. 10 Emission spectra of polymers I-IV in films cast from methanol at various excitation wavelengths

these solvents. These features strongly suggest that there existed less ordered structures in the solid-state morphology of these ionic polymers. Note here that both intra- and intermolecular π-π interactions of chromophores of polymers are mainly responsible for the ordered structures, which in turn usually cause λ_{em} to shift bathochromically to a great extent as 100 nm or higher and lower the quantum yields of light-emitting polymers in the solid state in general [31, 32]. These π-π interactions of chromophores were essentially minima in case of the conjugated polyp(pyridinium salt)s reported here. The light emission for each of these polymers occurred in green region in solutions and in the solid states.

Conclusions

Four conjugated poly(pyridinium salt)s were prepared from 3, 3′-dimethylnaphthidine and 4,4′-(1,4-phenylene)bis(2,6-diphenylpyrylium) tosylate by ring-transmutation polymerization and metathesis reactions. Their molecular structures and molecular weights were established by a combination of spectroscopic techniques and gel permeation chromatography. Their weight-average molecular weights (M_w) were in the range of 72–91 kg/mol and polydispersities in the range of 1.09–1.32. Their thermal stability is counterion dependent and is in the range of 290–425 °C as determined by thermogravimetric analyses. They also form counterion dependent lyotropic liquid-crystalline phases in organic solvents above their critical concentrations. Their optical properties evaluated by spectroflurometry show that each of these polymers emitted green light (500–572 nm) both in solutions and solid states.

Acknowledgments We thank the University of Houston-Downtown Department of Natural Sciences for the financial support of this project. Undergraduate student participant, DT was supported by Robert A. Welch Foundation's Departmental Grant (BJ-0027) to the University of Houston-Downtown. We sincerely thank Vinh Nguyen and Shaneela R. Omar for their initial contribution to this project. This work is in part supported by the NSF under Grant No. 0447416 (NSF EPSCoR RING-TRUE III), NSF-Small Business Innovation Research (SBIR) Award (Grant OII-0610753), NSF-STTR Phase I Grant No. IIP-0740289, and NASA GRC Contract No. NNX10CD25P.

Online Resources is available at http://www.nature.com/pj/index.html.

References

1. Bhowmik PK, Burchett RA, Han H, Cebe JJJ (2001) Polym Sci Part A: Polym Chem 39:2710
2. Bhowmik PK, Burchett RA, Han H, Cebe JJ (2001) Macromolecules 34:7579
3. Bhowmik PK, Burchett RA, Han H, Cebe JJ (2002) Polymer 43: 1953
4. Bhowmik PK, Han H, Cebe JJ, Nedeltchev IK, Kang S-W, Kumar S (2004) Macromolecules 37:2688
5. Bhowmik PK, Han H, Nedeltchev AKJ (2006) Polym Sci Part A: Polym Chem 44:1028
6. Bhowmik PK, Kamatam S, Han H, Nedeltchev AK (2008) Polymer 49:1748
7. Bhowmik PK, Han H, Nedeltchev AK, Mandal HD, Jimenez-Hernandez JA, McGannon PM (2009) Polymer 50:3128
8. Bhowmik PK, Han H, Nedeltchev AK, Mandal HD, Jimenez-Hernandez JA, McGannon PM (2010) J Appl Polym Sci 116:1197
9. Bhowmik PK, Han H, Nedeltchev AK (2006) Polymer 47:8281
10. Nedeltchev AK, Han H, Bhowmik PK (2010) Polym Chem 1:908
11. Nedeltchev AK, Han H, Bhowmik PKJ (2010) Polym Sci Part A: Polym Chem 48:4408
12. Nedeltchev AK, Han H, Bhowmik PKJ (2010) Polym Sci Part A: Polym Chem 48:4611
13. Nedeltchev AK, Han H, Bhowmik PKJ (2011) Polym Sci Part A: Polym Chem 49:1907
14. Jo TJ, Nedeltchev AK, Biswas B, Han H, Bhowmik PK (2012) Polymer 53:1063
15. Lu Y, Xiao C, Yu Z, Zeng X, Ren Y, Li C (2009) J Mater Chem 19: 8796
16. Han F, Lu Y, Zhang Q, Sun J, Zeng X, Li C (2012) J Mater Chem 22: 4106
17. Sun J, Lu Y, Wang L, Cheng D, Sun Y, Zeng X (2013) Polym Chem 4:4045
18. Jo TS, Han H, Ma L, Bhowmik PK (2011) Polym Chem 2:1953
19. Jo TS, Han H, Bhowmik PK, Ma L (2012) Macromol Chem Phys 213:1378
20. Ghanem BS, McKeown NB, Budd PM, Selbie JD, Fritsch D (2008) Adv Mater 20:2766
21. McKeown NB, Budd PM (2010) Macromolecules 43:5163

22. Rogan Y, Starannikova L, Ryzhikh V, Yampolskii Y, Bernado P, Bazzarelli F, Jansen JC, McKeown NB (2013) Polym Chem 4:3813
23. Rogan Y, Malpass-Evans R, Carta M, Lee M, Jansen JC, Bernardo P, Clarizia G, Tocci E, Friess K, Lanč M, McKeown NBJ (2014) Mater Chem A 2:4874
24. Cable KM, Mauritz KA, Moore RBJ (1995) Polym Sci Part A: Polym Chem 33:1065
25. Sander B, Tübke J, Wartewig S, Shaskov S (1996) Solid State Ionics 83:87
26. Bhowmik PK, Han H, Cebe JJ, Burchett RA, Sarker AMJ (2002) Polym Sci Part A: Polym Chem 40:659
27. Preston J (1982) Angew Makromol Chem 109/110:1
28. Bhowmik PK, Molla AH, Han H, Gangoda ME, Bose RN (1998) Macromolecules 31:621
29. Friend RH, Gymer RW, Holmes AB, Burroughes JH, Marks RN, Taliani C, Bradley DDC, Santos DAD, Bredas JL, Logdlund M, Salaneck WR (1999) Nature 397:121
30. Yeh KM, Lee CC, Chen YJ (2008) Polym Sci Part A: Polym Chem 46:5180
31. Sarker AM, Strehmel B, Neckers DC (1999) Macromolecules 32: 7409
32. Gettinger C, Heeger AJ, Drake J, Pine D (1994) J Chem Phys 101: 1673